

# Evaluation of Instability Criterion for Bidisperse Sedimentation

P. Maarten Biesheuvel and Henk Verweij

Laboratory for Inorganic Materials Science, Dept. of Chemical Technology & MESA Research Institute,  
University of Twente, P.O. Box 217, 7500 AE Enschede, The Netherlands

Victor Breedveld

Dept. of Chemical Engineering, University of California, Santa Barbara, CA 93106

*The instability criterion for bidisperse sedimentation derived by Batchelor and Janse van Rensburg was combined with two empirical models for the particle velocities that are consistent with conservation of momentum and used to construct theoretical stability diagrams. The stability boundaries were fully determined by the particle volume fractions, the particle-size ratio, and the ratio of the density differences with the liquid. The results showed that on increasing the particle-size ratio sufficiently, stability always is attained. For particles of similar size, instabilities occur mainly if the liquid density is intermediate between the particle densities. The stability diagrams agree well with the limited experimental data, if so-called "vertical columns" are excluded. This seems reasonable since similar structures observed in monodisperse suspensions are not captured by the bidisperse instability criterion either.*

## Introduction

The stability of initially homogeneous, bidisperse suspensions during sedimentation or creaming of the different particle species is important in several fields:

- Industrial solid-liquid separations (such as thickening and clarification) in which instabilities may result in an increased sedimentation rate (such as Weiland and McPherson, 1979)
- Industrial (hydraulic) classification for the separation of solid species according to size or density in chemical and mineral processing (Jean and Fan, 1986; Smith, 1997), in which instabilities may result in a decreased separation quality
- Material manufacturing by suspension processing (Biesheuvel et al., 1998) for which instabilities must be prevented to obtain a homogeneous sediment (Batchelor and Janse van Rensburg, 1986, p. 390).

Furthermore, as summarized by Huppert et al. (1991): "The fluid dynamics of convecting particulate suspensions is of great relevance to chemical and civil engineers, geologists, metallurgists and oceanographers. Diverse applications include the transport of soil, silt and sand in rivers and estuaries, volcanic flows of suspensions of hot air and ash, and the evolution of bodies of magma rich in crystals and impurities."

Whitmore (1955) first described that in bidisperse suspensions in which one of the particles is (close to) buoyant, homogeneous sedimentation—with clear horizontal boundaries—occurs below a certain critical volumetric concentration pair ( $\phi_1$ ,  $\phi_2$ ) while inhomogeneous structures are formed above this boundary. Weiland and coworkers used this effect to increase the initial settling rate by adding buoyant particles to a suspension, starting at their 1979 article. Batchelor and Janse van Rensburg (1986) gave the problem a solid theoretical footing and derived an elegant stability criterion based on vertical concentration fluctuations, given by

$$\left( \frac{\partial \phi_1 U_1}{\partial \phi_1} - \frac{\partial \phi_2 U_2}{\partial \phi_2} \right)^2 + 4\phi_1 \phi_2 \frac{\partial U_1}{\partial \phi_2} \frac{\partial U_2}{\partial \phi_1} < 0 \quad (1)$$

where  $U_i$  and  $\phi_i$  are the settling velocity and volume fraction of particle species  $i$ . If the criterion holds, unstable sedimentation is predicted with structure formation; if not, stable sedimentation occurs without the formation of lateral concentration gradients.

It is often noted that for suspensions in which one particle type sediments (settles down) and one creams (goes up), instabilities ('structure formation' or 'viscous fingering') will occur as a rule. When both particles sediment, Batchelor and

Correspondence concerning this article should be addressed to V. Breedveld.

Janse van Rensburg (1986) also observed instable sedimentation behavior at density ratios  $\gamma = (\rho_2 - \rho_0)(\rho_1 - \rho_0)^{-1}$  as high as  $\gamma = 0.7$ .

Cox (1990) derived a further criterion based on a horizontal concentration fluctuation, while Yan and Masliyah (1993) use Eq. 1 to describe several new measurements. Like Batchelor and Janse van Rensburg (1986), they use equations for  $U_i$ , derived by Batchelor (1982) that are correct to the order  $\phi_1 + \phi_2$  and proportional to the difference between particle density  $\rho_i$  and the liquid density  $\rho_0$ :  $U_i \propto (\rho_i - \rho_0)$ , which is not consistent with conservation of momentum. Therefore, this expression for  $U_i$  can only be applied in the dilute limit.

In this work, we will use two different models for the particle velocities in suspensions of particles of different size and density that are consistent with conservation of momentum in the concentrated regime. To our knowledge, no satisfactorily theoretical (microscopic) models are available for the sedimentation velocities in concentrated bidisperse suspensions. Therefore, we chose the empirical models of Masliyah (1979) and Patwardhan and Tien (1985) because these two models have predictive power in various experimental situations, as will be discussed in the next section. However, we want to emphasize that these expressions are empirical and lack a thorough microscopic background. The Masliyah model is considerably simpler than the Patwardhan and Tien model, but we investigated both models since there is insufficient experimental evidence in favor of either to justify leaving one out.

Using the models of Masliyah and Patwardhan and Tien, we will evaluate the criterion of Eq. 1 numerically to create stability diagrams. These diagrams are clarifying because they clearly show the practical conditions for instability and can be compared with experiments. To our knowledge, such diagrams were not constructed before from theory, most probably because former authors used expressions for  $U_i$  which are proportional to  $(\rho_i - \rho_0)$ . Yan and Masliyah (1993) indeed used these expressions for particle velocity and showed that no set  $(\phi_1, \phi_2)$  can be found for which instability is predicted.

## Theory

Simultaneous solution of the momentum equations for the liquid phase "0" and all particle phases "1...m" (Syamlal and O'Brien, 1988) results in the following expression for the particle velocities in multicomponent batch sedimentation (Patwardhan and Tien, 1985; Law et al., 1987; Biesheuvel, 2000a):

$$U_i = U_{i0} h_i \frac{\rho_i - \rho_s}{\rho_i - \rho_0} - \sum_{j=1}^m U_{j0} h_j \frac{\rho_j - \rho_s}{\rho_j - \rho_0} \phi_j. \quad (2)$$

For a large container (negligible wall effects) and laminar flow ( $Re < 0.2$ ), the particle velocity at infinite dilution  $U_{i0}$  is given by Stokes' law:

$$U_{i0} = \frac{d_i^2 (\rho_i - \rho_0) g}{18\eta} \quad (3)$$

with  $d_i$  the particle diameter,  $\rho_i$  the particle density,  $g$  gravity acceleration, and  $\eta$  the Newtonian viscosity of the liquid. The suspension density  $\rho_s$  is given by

$$\rho_s = (1 - \phi_{\text{tot}}) \rho_0 + \sum_{j=1}^m \phi_j \rho_j \quad (4)$$

$\phi_{\text{tot}}$  being the total particle concentration and  $\epsilon$  the liquid fraction

$$\phi_{\text{tot}} = \sum_{j=1}^m \phi_j, \quad \epsilon = 1 - \phi_{\text{tot}} \quad (5)$$

In deriving Eq. 2, the following assumptions are made:

- One-dimensional flow in direction of gravity, that is, no wall effects (see Tory et al., 1992) or lateral inhomogeneities
- Zero flux through any horizontal plane  $\sum_{j=1}^m \phi_j U_j + \epsilon U_0 = 0$  (with  $U_0$  the liquid velocity)
- Incompressible flow [ $\partial \phi_i / \partial t = 0$ ,  $\nabla \phi_i = 0$ ]
- Steady flow [ $\partial U_i / \partial t = 0$ ,  $\nabla U_i = 0$ ,  $i = 1 \dots m$ ]
- Absence of interparticle friction
- A constant interparticle stress (solids pressure,  $\nabla P_s = 0$ ).

The two models which will be investigated in this article only differ in their choice of the so-called hindrance function  $h_i$ . The Masliyah-model uses the Richardson-Zaki expression for  $h_i$

$$h_i = (1 - \phi_{\text{tot}})^{n_i - 2}. \quad (6)$$

For low Reynolds numbers and a high vessel size to particle-size ratio,  $n_i$  equals 4.65 (Wallis, 1969) and does not depend on the particle size; therefore, from this point forward,  $n$  without a subscript will be used.

Patwardhan and Tien incorporate a local particle concentration  $[1 + d_\epsilon/d_i]^{-3}$  in the hindrance function instead of  $\phi_{\text{tot}}$  to account for the different environment of particle species of different size

$$h_i = \left( 1 - \left( 1 + \frac{d_\epsilon}{d_i} \right)^{-3} \right)^{n-2}, \quad d_\epsilon = \frac{\sum_{j=1}^m d_j \phi_j}{\phi_{\text{tot}}} (\phi_{\text{tot}}^{-1/3} - 1). \quad (7)$$

For equal particle sizes, Eqs. 6 and 7 are equivalent. If all particles also have the same density (so that in fact a monodisperse suspension is obtained), both equations reduce to the classical Richardson-Zaki expression:

$$U_i = U_{i0} (1 - \phi_{\text{tot}})^n.$$

The above two models have been used extensively and with success to describe sedimentation and fluidization of a binary system in various experimental situations:

- Batch sedimentation with both particles sedimenting (Biesheuvel, 2000a, up to  $\phi_{\text{tot}} = 0.40$ ; Patwardhan and Tien, 1985, up to  $\phi_{\text{tot}} = 0.43$ ; Concha et al. (1992), up to  $\phi_{\text{tot}} = 0.25$ ; Lockett and Bassoon (1979), up to  $\phi_{\text{tot}} = 0.30$ )
- Batch settling with one particle sedimenting and one creaming (Law et al. (1987), up to  $\phi_{\text{tot}} = 0.16$ )

• Continuous gravity separations (Patwardhan and Tien, up to  $\phi_{\text{tot}} = 0.4$ ; Biesheuvel (2000b), up to  $\phi_{\text{tot}} = 0.18$ )

• Centrifugation (Biesheuvel and Verweij, 1999,  $\phi_{\text{tot}} = 0.20$ )

• Simultaneous filtration and sedimentation resulting in segregation (Biesheuvel, 2000a, up to  $\phi_{\text{tot}} = 0.18$ ).

Besides, these models have been applied to predict phase inversion for

• Liquid fluidized beds (Patwardhan and Tien, up to  $\phi_{\text{tot}} = 0.28$ )

• Batch sedimentation (Masliyah, 1979, at  $\phi_{\text{tot}} = 0.07$ ).

## Results and Discussion

### Explicit expressions for the differentials

For a bidisperse suspension, Eqs. 3–7 can be implemented in Eq. 2 to give expressions for particle velocities  $U_1$ ,  $U_2$  in terms of  $\phi_1$ ,  $\phi_2$ . To evaluate the instability criterion the four differentials in Eq. 1 must be derived. In order to save space, only two of the four differentials are presented here, because the other two can be derived in a straightforward manner by replacing each subscript “1” with a “2” and vice-versa.

For the Masliyah-model, the following expressions are obtained, when expressed in  $U_{10}$  and the densities  $\rho_0$ ,  $\rho_1$  and  $\rho_2$

$$\frac{\partial U_1}{\partial \phi_2} = \left( U_{10}(1 - \phi_1) \frac{\rho_0 - \rho_2}{\rho_1 - \rho_0} - U_{20} \left( \frac{\rho_2 - \rho_s}{\rho_2 - \rho_0} - \phi_2 \right) \right) \epsilon^{n-2} - (n-2) \left( U_{10}(1 - \phi_1) \frac{\rho_1 - \rho_s}{\rho_1 - \rho_0} - U_{20} \phi_2 \frac{\rho_2 - \rho_s}{\rho_2 - \rho_0} \right) \epsilon^{n-3} \quad (8)$$

$$\frac{\partial(U_1 \phi_1)}{\partial \phi_1} = \epsilon^{n-2} \left( U_{10} \frac{\rho_1 - \rho_s}{\rho_1 - \rho_0} (1 - 2\phi_1 - (1 - \phi_1)) \times (n-2) \phi_1 \epsilon^{-1} + U_{20} \frac{\rho_2 - \rho_s}{\rho_2 - \rho_0} ((n-2) \phi_1 \phi_2 \epsilon^{-1} - \phi_2) - U_{10}(1 - \phi_1) \phi_1 + U_{20} \phi_2 \phi_1 \frac{\rho_1 - \rho_0}{\rho_2 - \rho_0} \right) \quad (9)$$

For the Patwardhan and Tien model the resulting equations are more complex

$$\begin{aligned} \frac{\partial U_1}{\partial \phi_2} = & U_{10}(1 - \phi_1) \frac{\rho_0 - \rho_2}{\rho_1 - \rho_0} h_1 + U_{20} \phi_2 h_2 - U_{20} \frac{\rho_2 - \rho_s}{\rho_2 - \rho_0} h_2 \\ & + 3U_{10}(1 - \phi_1) \frac{\rho_1 - \rho_s}{\rho_1 - \rho_0} h_1^{(n-3)(n-2)} (n-2) \left( 1 + \frac{d_\epsilon}{d_1} \right)^{-4} \\ & \times \left( \frac{d_2}{d_1} \frac{\phi_{\text{tot}}^{-1/3} - 1}{\phi_{\text{tot}}} - \frac{d_\epsilon}{d_1 \phi_{\text{tot}}} - \frac{d_1 \phi_1 + d_2 \phi_2}{3d_1 \phi_{\text{tot}}^{7/3}} \right) \\ & - 3U_{20} \phi_2 \frac{\rho_2 - \rho_s}{\rho_2 - \rho_0} h_2^{(n-3)(n-2)} (n-2) \left( 1 + \frac{d_\epsilon}{d_2} \right)^{-4} \\ & \times \left( \frac{\phi_{\text{tot}}^{-1/3} - 1}{\phi_{\text{tot}}} - \frac{d_\epsilon}{d_2 \phi_{\text{tot}}} - \frac{d_1 \phi_1 + d_2 \phi_2}{3d_2 \phi_{\text{tot}}^{7/3}} \right) \quad (10) \end{aligned}$$

$$\begin{aligned} \frac{\partial(U_1 \phi_1)}{\partial \phi_1} = & \left( -U_{10} \frac{\rho_1 - \rho_s}{\rho_1 - \rho_0} h_1 - U_{20} \phi_2 \frac{\rho_0 - \rho_1}{\rho_2 - \rho_0} h_2 - U_{10} \right. \\ & \times (1 - \phi_1) h_1 \left. \right) \phi_1 + 3U_{10}(1 - \phi_1) \phi_1 \frac{\rho_1 - \rho_s}{\rho_1 - \rho_0} h_1^{(n-3)(n-2)} (n-2) \\ & \times \left( 1 + \frac{d_\epsilon}{d_1} \right)^{-4} \left( \frac{\phi_{\text{tot}}^{-1/3} - 1}{\phi_{\text{tot}}} - \frac{d_\epsilon}{d_1 \phi_{\text{tot}}} - \frac{d_1 \phi_1 + d_2 \phi_2}{3d_1 \phi_{\text{tot}}^{7/3}} \right) \\ & - 3U_{20} \phi_2 \phi_1 \frac{\rho_2 - \rho_s}{\rho_2 - \rho_0} h_2^{(n-3)(n-2)} (n-2) \left( 1 + \frac{d_\epsilon}{d_2} \right)^{-4} \\ & \times \left( \frac{d_1}{d_2} \frac{\phi_{\text{tot}}^{-1/3} - 1}{\phi_{\text{tot}}} - \frac{d_\epsilon}{d_2 \phi_{\text{tot}}} - \frac{d_1 \phi_1 + d_2 \phi_2}{3d_2 \phi_{\text{tot}}^{7/3}} \right) \\ & + U_{10}(1 - \phi_1) \frac{\rho_1 - \rho_s}{\rho_1 - \rho_0} h_1 - U_{20} \phi_2 \frac{\rho_2 - \rho_s}{\rho_2 - \rho_0} h_2 \quad (11) \end{aligned}$$

From this point forward, we use the following parameters to evaluate the results: the density ratio  $\gamma = (\rho_2 - \rho_0)(\rho_1 - \rho_0)^{-1}$  and the particle-size ratio  $\lambda = d_2 d_1^{-1}$ . Note that  $\gamma < 0$  means that one of the particle species is lighter than the liquid and the other heavier; for  $\gamma = -1$  the density differences with the liquid are equal. As noted before, for  $\lambda = 1$ , the outcome of the Masliyah- and the Patwardhan and Tien models are the same. Eqs. 8–11 can be expressed in  $\gamma$  and  $\lambda$  using the following conversions:

$$\begin{aligned} \frac{\rho_2 - \rho_s}{\rho_2 - \rho_0} &= 1 - \phi_2 - \phi_1 \gamma^{-1}, \quad \frac{\rho_1 - \rho_s}{\rho_1 - \rho_0} = 1 - \phi_1 - \phi_2 \gamma \\ \frac{d_\epsilon}{d_1} &= (\phi_1 + \lambda \phi_2) \phi_{\text{tot}}^{-1} (\phi_{\text{tot}}^{-1/3} - 1), \\ \frac{d_\epsilon}{d_2} &= (\lambda^{-1} \phi_1 + \phi_2) \phi_{\text{tot}}^{-1} (\phi_{\text{tot}}^{-1/3} - 1) \quad (12) \end{aligned}$$

For the Masliyah model the expressions in terms of  $\gamma$  and  $\lambda$  are as follows:

$$\begin{aligned} \frac{\partial}{\partial \phi_2} \frac{U_1}{U_{10}} = & \left[ -(1 - \phi_1) \gamma - \lambda^2 \gamma (1 - 2\phi_2 - \phi_1 \gamma^{-1}) \right] \epsilon^{n-2} \\ & - (n-2) \left[ (1 - \phi_1) (1 - \phi_1 - \phi_2 \gamma) - \lambda^2 \gamma \phi_2 (1 - \phi_2 - \phi_1 \gamma^{-1}) \right] \\ & \times \epsilon^{n-3} \quad (13) \end{aligned}$$

$$\begin{aligned} \frac{\partial}{\partial \phi_1} \frac{U_1 \phi_1}{U_{10}} = & \epsilon^{n-2} \left\{ (1 - \phi_1 - \phi_2 \gamma) [1 - 2\phi_1 - (1 - \phi_1)(n-2) \right. \\ & \times \phi_1 \epsilon^{-1}] + \lambda^2 \gamma (1 - \phi_2 - \phi_1 \gamma^{-1}) [(n-2) \phi_1 \phi_2 \epsilon^{-1} - \phi_2] \\ & \left. - (1 - \phi_1) \phi_1 + \lambda^2 \phi_2 \phi_1 \right\} \quad (14) \end{aligned}$$

Note that  $U_{10}$  will drop out of the criterion 1 when all four differentials are implemented. Equations 13 and 14 cannot simply be rewritten to give  $(\partial U_2 / \partial \phi_1) = f(\gamma, \lambda)$  and  $[\partial(U_2 \phi_2) / \partial \phi_2] = f(\gamma, \lambda)$ . These differentials can best be obtained via Eqs. 8 and 9 by interchanging subscripts “1” and “2.” For the Patwardhan and Tien model the four differentials in terms of  $\gamma$  and  $\lambda$  are rather bulky and therefore not presented here.

## Numerical technique

The criterion 1 is evaluated by an iterative technique using the built-in 'solver' of a commercial software package (Excel 7.0, Microsoft, Richmond, VA). The solver uses a Newton iteration scheme and for proper convergence we used a precision of  $10^{-22}$ , a tolerance of 0.1% and a convergence of  $10^{-9}$ .

## Generality of numerical results

Batchelor and Janse van Rensburg (1986) state (p. 383, 403) that each bidispersion is specified by  $\phi_1$ ,  $\phi_2$ ,  $\gamma$  and  $\lambda$ , which may be obvious for their particle transport model based on  $U_i \propto U_{i0}$ . Equations 8–12 show that also for the Masliyah- and Patwardhan and Tien-model, Eq. 1 is uniquely specified by the parameters  $\phi_1$ ,  $\phi_2$ ,  $\gamma$ ,  $\lambda$  (and  $n$ ). This is important because it implies that the results presented in the figures in this work are general for the two parameters in the captions (with  $n$  always 4.65).

In the following subsections, the results will be shown for a number of special parameter settings to enable comparison with the available experimental data and to provide insight into the full predictive power of the instability criterion.

## Calculations and experiments for $\gamma = -1$ and $\lambda = 1$

The stability boundary for  $\gamma = -1$  and  $\lambda = 1$  is presented in Figure 1 and compared with experiments by Batchelor and Janse van Rensburg's (1986). We used the data from Batchelor and Janse van Rensburg's (1986) Table 4, which, for the system B2, is in slight disagreement with their Figure 6 ( $\phi_1 = 0.23$  vs. 0.25).

For  $\lambda = 1$  and  $\gamma = -1$ , the stability of a system (either data points or the simulated boundary) is invariant under the exchange of  $\phi_1$  and  $\phi_2$ , so we only need to consider the area

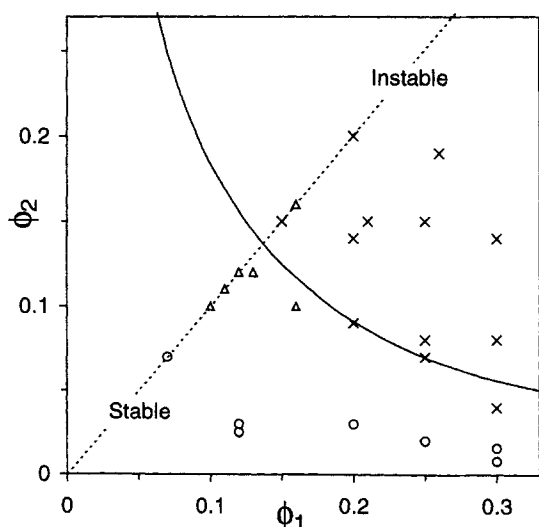


**Figure 1. Instability diagram for  $\lambda = 1$  and  $\gamma = -1$ .**

Measurements from Batchelor and Janse van Rensburg's (1986) Tables 3 and 4 and Figure 6; O: stable; Δ: type C instability (vertical columns); x: types B, BC and CB instabilities. Marginally stable measurements are not shown. The stability boundary for  $\lambda = 1.03$  (system C) is practically the same as for  $\lambda = 1$ .

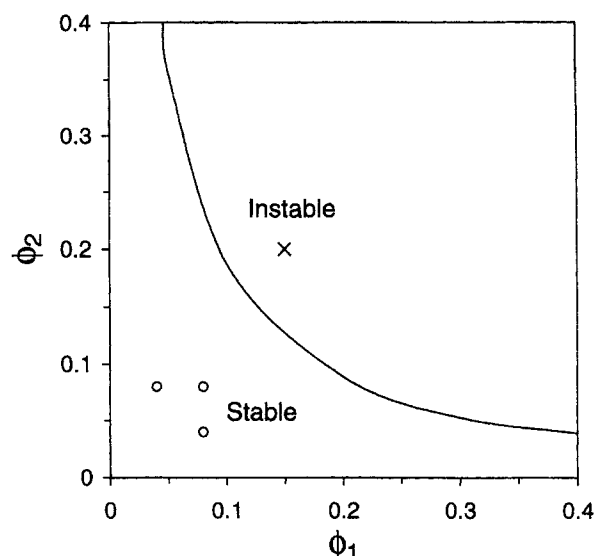


**Figure 2. Instability diagram for  $\lambda = 0.98$  and  $\gamma = -0.94$ .**

Measurements from Law et al. (1987) (1 = PS, 2 = PMMA,  $\rho_1 = 1,050 \text{ kg/m}^3$ ,  $d_1 = 241 \text{ μm}$ ,  $\rho_2 = 1,186 \text{ kg/m}^3$ ,  $d_2 = 237 \text{ μm}$ ). The stability boundary is similar for both the Patwardhan and Tien and the Masliyah model, since  $\lambda \approx 1$ .

below the 1:1-line. The rest of the graph can be constructed using this symmetry.

For  $\lambda = 1$ ,  $\gamma = -1$  an instability boundary exists in accordance with Batchelor and Janse van Rensburg's (1986) belief (p. 399) that "the condition for instability is satisfied for some values of  $\phi_1$  and  $\phi_2$  when  $\lambda = 1$ ,  $\gamma = -1$ ." The stability boundary accurately predicts the experimentally observed stability behavior if we only consider B, BC and CB types of instability structures, but not the type C vertical columns. This suggests that these latter instabilities are caused by another mechanism than quantified in criterion (1). This hypothesis is supported by the observation of "streaming effects" by Whitmore (1955)—similar to Batchelor and Janse van Rensburg's (1986) vertical columns—in a monocomponent suspension of  $\phi > 0.15$  which are not predicted by the monodisperse limit of Eq. 1 either (see next section).

The few observations made by Law et al. (1987) on stability in bidisperse sedimentation for  $\gamma = -1$  and  $\lambda = 1$  are summarized in Figure 2 and are in good agreement with both the Masliyah- and the Patwardhan and Tien model.

## Calculations for different $\gamma$ and $\lambda$ values

The symmetry around the 1:1-line is broken if either  $\gamma \neq -1$  or  $\lambda \neq 1$  as shown in Figure 3 and Figure 4. Figure 3a shows that for the Masliyah-model the instability region does not simply consist of the 'upper right'-side of the diagram but that for  $\lambda$  values below  $\sim 0.2$  (and thus above  $\sim 5$ , since the indices 1 and 2 can be transposed), an instability region is obtained with stability 'on both sides.'

For the Patwardhan and Tien model (Figure 3b) and for  $\lambda \leq 0.2$ , the instability boundary shifts to higher  $\phi_1$ -values than for the Masliyah-model, while the 'vertical symmetry' is lost completely.

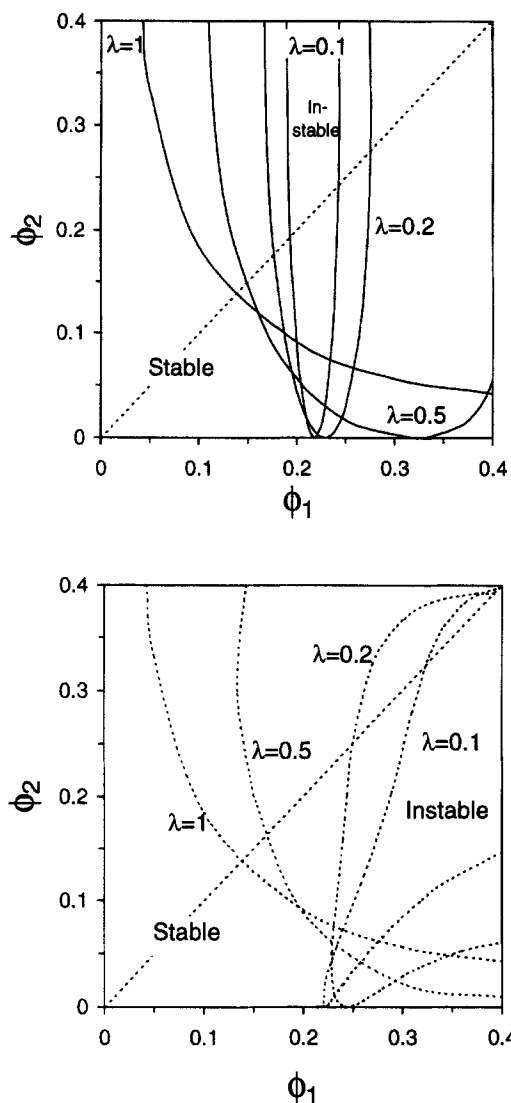


**Figure 3. Instability diagram for  $\gamma = -1$  and different  $\lambda$ -values.**

By exchanging  $\phi_1$  and  $\phi_2$ , the contours for  $\lambda = 2, 5$  and  $10$  are obtained. Solid lines, Masliyah-model; dashed lines, Patwardhan and Tien-model.

Both in Figure 3 and Figure 4, the instability boundary approaches the  $x$ -axis ( $\phi_2 = 0$ ) for several values of  $\gamma$ ,  $\lambda$  and  $\phi_1$ , which suggests that under these conditions no stable bidisperse suspension exists.

From numerical solution of Eq. 1, we could not find out whether  $\phi_2 = 0$  is actually reached, because convergence of Eq. 1 at low  $\phi_1$ -values was problematic. Therefore, we derived an analytic expression for  $\phi_1$  with  $\phi_2 = 0$  based on Eq. 1 and the Masliyah-model, which results in

$$\phi_1^* = \frac{n+1-\lambda^2 - \sqrt{(n+1-\lambda^2)^2 - 4n(1-\gamma\lambda^2)}}{2n} \quad (15)$$

Equation 15 gives a single solution for  $\phi_1^*$  for each set of ( $\gamma$ ,  $\lambda$ ,  $n$ ). The solutions for  $\lambda = 0.5, 0.2$  and  $0.1$  ( $n = 4.65$ ,  $\gamma = -1$ )

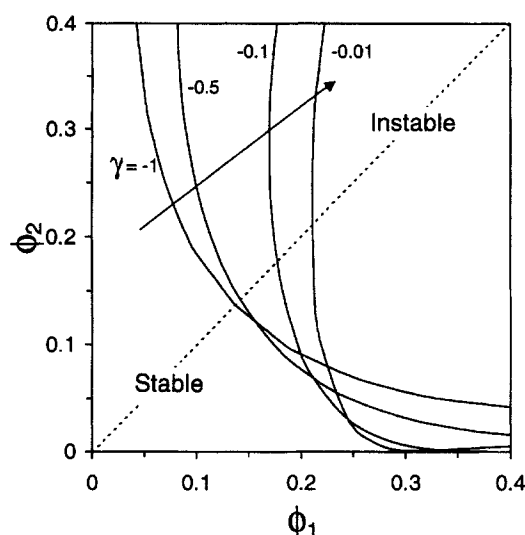


**Figure 4. Instability diagram for  $\lambda = 1$  and different  $\gamma$  values.**

$\gamma$  decreases in direction of the arrow ( $\gamma = -1, -0.5, -0.1$  and  $-0.01$ ). By exchanging  $\phi_1$  and  $\phi_2$ , the contours for  $\gamma = -2, -10$  and  $-100$  are obtained.

are in agreement with Figure 3a ( $\phi_1 = 0.319, 0.229$  and  $0.218$ , respectively).

This analysis shows that a mono-component suspension is stable (lefthand side of Eq. 1  $< 0$ ) for all  $\phi_1$  except for  $\phi_1^*$  in which case stability is undefined. This conclusion is in agreement with Batchelor and Janse van Rensburg's (1986) remarks that (p. 398) "...all bidispersions are stable when either  $\phi_1$  or  $\phi_2$  is sufficiently small" and (p. 403) "We saw that  $I$  (Eq. 1) approaches a positive limit as either  $\phi_1 \rightarrow 0$  or  $\phi_2 \rightarrow 0$ , indicating stability near the  $\phi_1$  and  $\phi_2$  axes in Figure 6, in accordance with the data," but note that for  $\phi_1$  near  $\phi_1^*$ , "sufficiently small" may indeed be very small, such as for  $\gamma = -1$ ,  $\lambda = 0.2$  and  $\phi_1 = 0.235$ , stability is attained only for  $\phi_2 < 2.3 \times 10^{-3}$ .

#### Calculations for $\phi_1 = \phi_2$

For comparison of the theoretical predictions for different  $\lambda$ - and  $\gamma$ -values as presented in Figure 3 and Figure 4 with experimental data, we have carried out additional calculations for the specific case  $\phi_1 = \phi_2$ . Batchelor and Janse van Rensburg (1986) have performed experiments in this regime ( $\phi_1 = \phi_2 = 0.15$ ;  $-0.67 < \gamma < 0.95$  and  $0.38 < \lambda < 2.56$ ). They observed a region of instability that extended to  $\gamma \sim 0.7$  for  $\lambda$  around unity. For both lower and higher values of  $\lambda$  the stability boundary is shifted to lower values of  $\gamma$ , giving rise to an ellipsoidal shape of the stability boundary in a  $\lambda$ - $\gamma$  plot (see their Figure 7). We present results of our calculations in a similar diagram for different values of  $\phi_1 = \phi_2$  in Figure 5. This figure—with a linear  $\gamma$ -axis—contains all necessary data for the four cases evaluated (namely  $\phi_1 = \phi_2 = 0.15, 0.175, 0.2$  and  $0.225$ ). When compared with the Masliyah-model, the Patwardhan and Tien model predicts that the region of instability extends more toward positive  $\gamma$ -values but extends less from the  $\lambda = 1$  axis. As can be observed in Figure 5, both models give the same result for  $\lambda = 1$ , as is expected because for equal particle sizes the hindrance factor (Eq. 7) equals

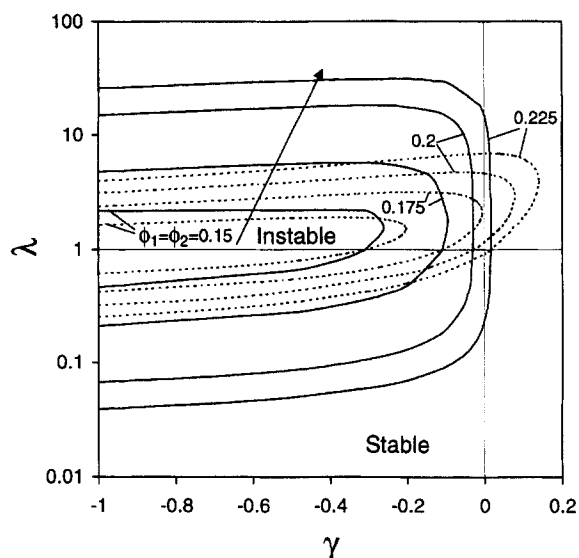


**Figure 5. Instability diagram for  $\phi_1 = \phi_2$ .**

Masliyah-model (solid lines) and Patwardhan and Tien-model (dashed lines) for increasing  $\phi_1 = \phi_2$  in the direction of the arrow (0.15, 0.175, 0.2 and 0.225, respectively).

(Eq. 6). For  $\gamma = -1$ , the two  $\lambda$  values are related by  $\lambda_1 = 1/\lambda_2$  while the tangents at  $(\gamma_1, \lambda_1)$  and  $(\gamma_2, \lambda_2)$  are parallel in a  $[\log(\lambda) - \gamma]$  diagram as noted by Batchelor and Janse van Rensburg (1986) (p. 392) “owing to the invariance of these systems under the interchange  $\gamma \rightarrow 1/\gamma$ ,  $\lambda \rightarrow 1/\lambda$ , the stability boundary must cut the line  $\gamma = -1$  at points equidistant from  $\lambda = 1$  and with parallel tangents at these two points.”

To form a clear picture of the instability boundaries, two more plots are constructed with logarithmic  $\gamma$ -axes; Figure 6a describes negative  $\gamma$ -values and Figure 6b positive  $\gamma$ -values. For  $\phi_1, \phi_2 > 0.137$ , a region of instability exists (see Figure 1), while the point  $(\gamma = -1, \lambda = 1)$  is always within this region and is the point of symmetry for the  $\gamma < 0$ -part of the instability boundary (Figure 6a). For these points, one-half of the boundary can be derived from the other half by using the conversions  $\lambda_2 = 1/\lambda_1$ ;  $\gamma_2 = 1/\gamma_1$ . For low enough  $\phi_1, \phi_2$  (that is,  $< 0.21$  for the Masliyah-model and  $< 0.18$  for the Patwardhan and Tien model), each instability boundary is a closed line surrounding a single region of instability (Figure 6a). However, if the contour intersects  $\gamma = 0$ , it will also extend to  $+\infty$  and to  $-\infty$  (Figure 6b), while two regions of instability are formed at the positive  $\gamma$ -axis. The two parts of the contour at  $\gamma > 0$  mirror in the point  $(\gamma = 1, \lambda = 1)$ ; this point always lies outside the instability region, which is not surprising since it represents the monodisperse case (identical size and density). We now compare the results of Figure 5 and Figure 6 with several experimental findings and theoretical considerations:

According to Figure 5, instabilities are predicted for systems with  $\gamma < 0$ , which is in agreement with the experiments by Weiland and McPherson (1979) on the increase in settling velocity if a settler is aerated (see Introduction).

Instabilities at positive  $\gamma$  are predicted at high concentrations ( $\phi_1, \phi_2 > 0.21$  of the Masliyah-model and  $\phi_1, \phi_2 > 0.18$  for the Patwardhan and Tien model) and for particles of the

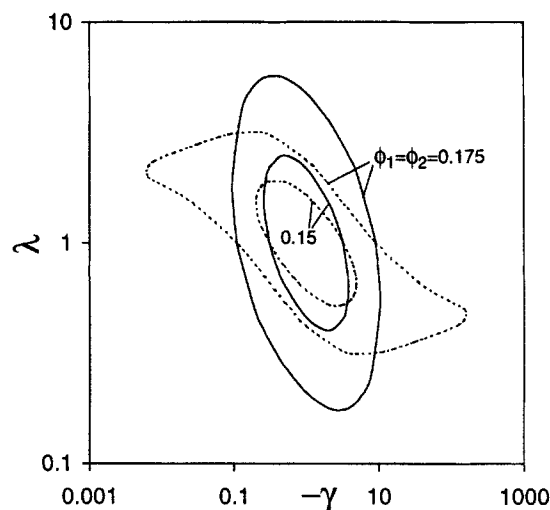


**Figure 6a. Instability diagram for  $\phi_1 = \phi_2$ .**

Masliyah model (solid lines) and Patwardhan and Tien model (dashed lines), for increasing  $\phi_1 = \phi_2$  (0.15 and 0.175, respectively) moving outward from the center ( $-\gamma = \lambda = 1$ ).

same size order ( $0.1 < \lambda < 10$  for the Masliyah-model and  $1 < \lambda < 10$  for the Patwardhan and Tien-model), which is in agreement with Batchelor and Janse van Rensburg's (1986) tentative remark (p. 401) that “the possibility of instability when  $\gamma > 0$  may exist at large values of  $\phi_1$  and  $\phi_2$ .”

For a sufficiently high particle-size ratio (such as  $\lambda < 0.1$  and  $\lambda > 10$ ), stable sedimentation is predicted by both models (up to  $\phi_{\text{tot}} = 0.45$ ), in agreement with Batchelor and Janse van Rensburg's (1986) conclusion (p. 402) that “... the dispersion is stable when the spheres of one species are much smaller than those of the other species, for any value of the density ratio  $\gamma$  and for any values of the volume fractions  $\phi_1$  and  $\phi_2$ .”

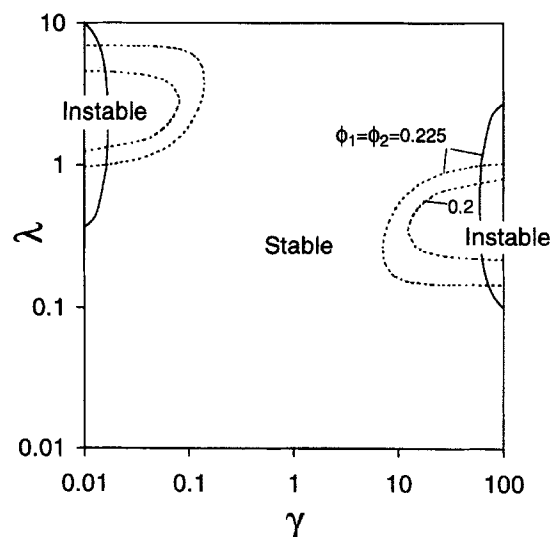


**Figure 6b. Instability diagram for  $\phi_1 = \phi_2$ .**

Masliyah-model (solid line,  $\phi_1 = \phi_2 = 0.225$ ) and Patwardhan and Tien model (dashed lines,  $\phi_1 = \phi_2 = 0.2$  and  $\phi_1 = \phi_2 = 0.225$ ).

The measurements by Batchelor and Janse van Rensburg (1986; Table 5, Figure 7) on which our Figure 5 is based show instabilities ("large scale structures," p. 390) at considerably higher density ratios  $\gamma$  than predicted by the models. A similar discrepancy was found in Figure 1, where we have shown that the stability boundaries of the empirical models are in good agreement with the experiments if the type C structures (vertical columns) are not considered unstable. Though Batchelor and Janse van Rensburg (1986) do not explicitly specify the instability type for the experiments presented in their Figure 7, an analysis of their other experimental data makes it plausible to assume that indeed type C was the dominant structure in these experiments:

(1) Batchelor and Janse van Rensburg's (1986) Figure 7 is based on  $\phi_1 = \phi_2 = 0.15$  which according to their Figure 6 is close to the region of vertical columns.

(2) Batchelor and Janse van Rensburg (1986) remark (p. 392) that "the grains ... were ... very weakly formed" and "...some repetition and refinement [were necessary] to determine whether a given system was stable or not" which agrees with the observed poor contrast for vertical columns (Batchelor and Janse van Rensburg's (1986) Figure 6).

If this is not the case, we suppose that the observed instabilities in Batchelor and Janse van Rensburg's (1986) Figure 7 are caused by another mechanism than quantified in Eq. 1. Though Cox (1990) assumes that the (initial) instability of a bidisperse suspension is described by one and only one mechanism (either by the variation of  $\phi_1$ ,  $\phi_2$  in vertical direction, as considered by Batchelor and Janse van Rensburg (1986), by a variation in horizontal direction, as considered by Cox, or by another variation), it is also possible that different instability types are caused by different mechanisms with different criteria.

With respect to the tests with  $\phi_1 = \phi_2 = 0.15$ , Batchelor and Janse van Rensburg (1986) note "the observed stability of a mixture of any two sizes of particles made of the same material when  $\phi_1 = \phi_2 = 0.15$  is also noteworthy from a practical viewpoint, and it would be useful to know if the same is true at other concentrations." Figure 6b shows that for  $\phi_1 = \phi_2$  and  $\phi_{\text{tot}} \leq 0.45$ , sedimentation is stable in a broad region around  $\gamma = 1$  for all  $\lambda$  values. To investigate other ( $\phi_1$ ,  $\phi_2$ )-sets, we performed calculations at  $\gamma = 1$  ( $\rho_1 = \rho_2$ ) at  $\lambda = 0.1$ , 1, 3 and 10 and at  $\phi_1 = 0.01, 0.05, 0.1, 0.2$  and 0.4 (all combinations). No  $\phi_2$ -values were found for which Eq. 1 holds, suggesting that stable sedimentation always occurs for  $\gamma = 1$ . This is in agreement with experiments by many authors who studied sedimentation of particles of the same material but with different sizes and who never reported instabilities and often explicitly mentioned stable sedimentation with clearly visible horizontal interfaces (Smith (1965), number of species  $m = 2$ ; Smith (1966),  $m = 4$ ; Davies (1968, 1969),  $m = 2, 3$ ; Davies and Kaye (1971, 1972),  $m = 2$ ; Lockett and Al-Habbooby (1973),  $m = 2, 3$ ; Lockett and Bassoon (1979),  $m = 2$ ; Mirza and Richardson (1979),  $m = 2$ ; Schneider et al. (1985),  $m = 2$ ; Davis and Hassen (1988),  $m = \infty$ ; Biesheuvel (2000a),  $m = 2$ ).

Although many of the above results seem curious, such as a stable region at high  $\phi_1$  for  $\lambda < 0.2$ ,  $\gamma = -1$  (Figure 3) and an instable region for  $(\phi_1 = \phi_2) > 0.2$ ,  $\gamma > 13$ ,  $\lambda \sim 0.33$  (Figure 6b), we see no reason to doubt the calculations as long as we accept Eqs. 1, 2 and Eqs. 6 and 7. Based on the instability

diagrams, many experiments can be devised to validate or falsify the presented set of equations.

## Conclusions

Combining the criterion for stability in bidisperse suspensions derived by Batchelor and Janse van Rensburg (1986) with the empirical particle velocity models by Masliyah (1979) and Patwardhan and Tien (1985) yields valuable information on the influence of particle size ratio  $\lambda$ , density ratio  $\gamma$  and particle volume fractions  $\phi_1$  and  $\phi_2$  on suspension stability. Stability diagrams could be constructed as a function of these parameters. This in contrast to the dilute limit particle velocity model of Batchelor (1982), which does not predict instability in bidisperse suspensions under the circumstances considered by Yan and Masliyah (1993). Apparently, the concentration effects are vital to capture the physics of suspension instability.

From the stability diagrams it can be concluded that for all parameter settings minimum concentration values exist below which the suspension is stable. On increasing the particle concentrations, instabilities occur first for suspensions in which the liquid density is intermediate between the densities of both particle species (that is,  $\gamma < 0$ , so that one species creams and the other settles), with the particle size ratio between 0.1 and 10. For highly concentrated systems, the instable region extends to positive values for  $\gamma$ , so that instability is expected for systems in which both particles are heavier (or lighter) than the suspending fluid.

The limited experimental results that could be found were in good agreement with the predictions of the model. The main discrepancy was found for the "column-like" structures of Batchelor and Janse van Rensburg (1986). The points associated with such structures were located in the stable region as predicted by the models. Whitmore (1955) has observed similar structures in monodisperse suspensions, which at least suggests that the instabilities as detected by Batchelor and Janse van Rensburg are not due to the bidispersity of the suspensions but that some other mechanism exists which is not captured by the bidisperse instability criterion. If the column-like structures are left out of the stability diagrams, the agreement with the model predictions is very good.

Clearly, more experiments are required to test the stability criterion and discriminate between the empirical models of Masliyah (1979) and Patwardhan and Tien (1985) evaluated in this article, for which the stability diagrams in this article can be used as a starting point.

## Literature Cited

- Batchelor, G. K., "Sedimentation in a Dilute Polydisperse System of Interacting Spheres. Part 1. General Theory," *J. Fluid Mech.*, **119**, 379 (1982).
- Batchelor, G. K., and R. W. Janse van Rensburg, "Structure Formation in Bidisperse Sedimentation," *J. Fluid Mech.*, **166**, 379 (1986).
- Biesheuvel, P. M., A. Nijmeijer, and H. Verweij, "Theory of Batchwise Centrifugal Casting," *AIChE J.*, **44**, 1914 (1998).
- Biesheuvel, P. M., and H. Verweij, "Calculation of the Composition Profile of a Functionally Graded Material Produced by Centrifugal Casting," *J. Am. Ceram. Soc.*, **83**, 743 (2000).
- Biesheuvel, P. M., "Particle Segregation during Pressure Filtration for Cast Formation," *Chem. Eng. Sci.*, **55**, 2595 (2000a).

- Biesheuvel, P. M., "Comments on 'A Generalized Empirical Description for Particle Slip Velocities in Liquid Fluidized Beds,'" *Chem. Eng. Sci.*, **55**, 1945 (2000b).
- Concha, F., C. H. Lee, and L. G. Austin, "Settling Velocities of Particulate Systems. 8. Batch Sedimentation of Polydispersed Suspensions of Spheres," *Int. J. Miner. Process.*, **35**, 159 (1992).
- Cox, R. G., "Instability of Sedimenting Bidisperse Suspensions," *Int. J. Multiphase Flow*, **16**, 617 (1990).
- Davies, R., "The Experimental Study of the Differential Settling of Particles in Suspension at High Concentrations," *Powder Techn.*, **5**, 43 (1968-69).
- Davies, R., and B. H. Kaye, "Experimental Investigation into the Settling Behavior of Suspensions," *Powder Techn.*, **5**, 61 (1971-1972).
- Davis, R. H., and M. A. Hassen, "Spreading of the Interface at the Top of a Slightly Polydisperse Sedimenting Suspension," *J. Fluid Mech.*, **196**, 107 (1988).
- Huppert, H. E., R. C. Kerr, J. R. Lister, and J. S. Turner, "Convection and Particle Entrainment Driven by Differential Sedimentation," *J. Fluid Mech.*, **226**, 349 (1991).
- Jean, R.-H., and L.-S. Fan, "On the Criteria of Solids Layer Inversion in a Liquid-Solid Fluidized Bed Containing a Binary Mixture of Particles," *Chem. Eng. Sci.*, **41**, 2811 (1986).
- Law, H.-S., J. H. Masliyah, R. S. MacTaggart, and K. Nandakumar, "Gravity Separation of Bidisperse Suspensions: Light and Heavy Particle Species," *Chem. Eng. Sci.*, **42**, 1527 (1987).
- Lockett, M. J., and H. M. Al-Habbooby, "Differential Settling by Size of Two Particle Species in a Liquid," *Trans. Instn. Chem. Engrs.*, **51**, 281 (1973).
- Lockett, M. J., and K. S. Bassoon, "Sedimentation of Binary Mixtures," *Powder Technol.*, **24**, 1 (1979).
- Masliyah, J. H., "Hindered Settling in a Multi-Species Particle System," *Chem. Eng. Sci.*, **34**, 1166 (1979).
- Mirza, S., and J. F. Richardson, "Sedimentation of Suspensions of Particles of Two or More Sizes," *Chem. Eng. Sci.*, **34**, 447 (1979).
- Patwardhan, V. S., and C. Tien, "Sedimentation and Liquid Fluidization of Solid Particles of Different Sizes and Densities," *Chem. Eng. Sci.*, **40**, 1051 (1985).
- Schneider, W., G. Anestis, and U. Schaflinger, "Sediment Composition Due to Settling of Particles of Different Sizes," *Int. J. Multiphase Flow*, **11**, 419 (1985).
- Smith, T. N., "The Differential Sedimentation of Two Different Species," *Trans. Instn. Chem. Engrs.*, **43**, T69-73 (1965).
- Smith, T. N., "The Sedimentation of Particles Having a Dispersion of Sizes," *Trans. Instn. Chem. Engrs.*, **44**, T153 (1966).
- Smith, T. N., "Differential Settling of a Binary Mixture," *Powder Techn.*, **92**, 171 (1997).
- Syamlal, M., and T. J. O'Brien, "Simulation of Granular Layer Inversion in Liquid Fluidized Beds," *Int. J. Multiphase Flow*, **14**, 473 (1988).
- Tory, E. M., M. T. Kamel, and C. F. Chan Man Fong, "Sedimentation is Container-Size Dependent," *Powder Techn.*, **73**, 219 (1992).
- Wallis, G. B., *One-Dimensional Two-Phase Flow*, McGraw-Hill, New York (1969).
- Weiland, R. H., and R. R. McPherson, "Accelerated Settling by Addition of Buoyant Particles," *Ind. Eng. Chem. Fundam.*, **18**, 45 (1979).
- Yan, Y., and J. H. Masliyah, "Sedimentation of Solid Particles in Oil-in-Water Emulsions," *Int. J. Multiphase Flow*, **19**, 875 (1993).

Manuscript received Nov. 2, 1999, and revision received Apr. 14, 2000.